Modified Space Vector Modulated Matrix Converter with Supply Current Quality Improvement under Unbalanced Supply Conditions

Payal Patel, and Mahmadasraf A. Mulla, *Senior Member, IEEE,*

***Abstract*—In this work, a new input current modulation technique is presented for the matrix converter (MC) working in the conditions of unbalanced supply. The proposed technique improves the quality of the supply currents when the output performance of the MC is improved by considering the actual supply voltage characteristics in the SVM technique. While the balanced output voltages are produced by SVM technique under unbalanced supply voltage condition, the MC input performance is degraded due to the injection of harmonics with the low frequencies in the supply currents. In this condition, the supply current quality is upgraded by modifying the input modulation vector based on the positive/negative sequence components of the supply voltages. The approaches adopted by the existing input current modulation techniques to decompose the positive/negative sequence components are complex and require large storage space. This drawback is overcome in the presented technique by using the instantaneous power theory to derive the input current modulation vector based on the positive sequence components of the supply voltages. The presented technique of deriving input modulation vector does not require the complex and memory consuming sequence decomposition methods and therefore can be realized easily as compared to existing input modulation techniques of the MC. The effectuality of the new technique is confirmed by the results of simulation performed in PSIM software and real time results in OPAL-RT. Comparison of the presented technique is carried out with two other techniques to show the effectiveness.**

***Index Terms*—Harmonics, input current modulation, matrix converter, space vector modulation, THD.**

I. Introduction

THE matrix converter (MC) is a single stage AC-AC power conversion device which is able to produce the variable voltage with the variable frequency. Some distinct features of the MC are sinusoidal input/output waveforms, four quadrant operation, adjustable power factor, long life with compact size due to the absence of energy storing element [1][2][3][4]. Despite of having many advantages, the MC suffers from the several limitations which hinder its full acceptance by the industry. The limitations of the MC are complexity of controlling nine bidirectional switches, limited voltage transfer ratio, sensitivity to the input disturbances, complicated commutation and protection etc.

Practically, the input voltages to the MC become unbalanced and/or distorted due to the large number of asymmetric and nonlinear loads connected to the supply grid. Therefore, it becomes necessary to examine the MC performance under such an abnormal input voltage conditions. In the MC, due to the absence of energy storing element, the output performance is highly degraded in the presence of unbalanced and/or distorted power supplies [5]. In the literature, several modified modulation techniques for the MC are suggested to eliminate the effects of unbalance/distortion present in the input voltages on the MC output voltages[6], [7], [8], [9], [10], [11], [12], [13]. In [6] [7], the conventional Alesina-Venturini modulation technique of the MC is modified to produce the required output voltages by calculating the duty ratios using the actual supply voltages. The MC output performance is enhanced by close loop control of the output currents in [8]. Most widely used space vector modulation (SVM) strategy for the MC is modified in [9], [10], [11], [12], [13] for producing the balanced load voltages from the abnormal supply. The output performance of the MC is improved in [9] by modifying the modulation vector of the fictitious rectifier stage of the MC based on the negative sequence components of the supply voltages. Feedback and Feed-forward modulation techniques are presented in [10][11] to refine the output performance of the MC with the unbalance present in the supply voltages. In [12][13], the required output performances of the MC are obtained by considering the real supply voltages for the calculations of the input modulation angle and modulation index of the SVM technique.

However, the above modulation techniques which upgrade the MC output performance in the presence of unbalanced input voltages, degrades the input performance. Considerable amount of lower order harmonics are injected into the supply currents whilst balanced output voltages are generated by the MC with the unbalanced supply [14]. With the purpose of improving the supply current quality in the presence of supply voltage unbalance, several input current modulation techniques are suggested in the literature [15], [16], [17], [18], [19].

The dynamic modulation technique presented in [14], [15], [16], [17] modifies the input modulation vector of the MC based on the positive and negative sequence components of the supply voltages. The input current modulation technique suggested in [18], modifies the input modulation vector using the positive sequence components of the supply voltages. A notch filter based simplified technique is proposed in [20] which overcomes the realization difficulties associated with the above input current modulation methods. The supply currents in [21] are improved by using the feedback control loops on the input side of the MC. The method uses the resonant controllers to regulate the input active power and

Manuscript received July 1, 2020; revised November 6, 2020.

Mahmadasraf A. Mulla is with the Department of Electrical Engineering, S. V. National Institute of Technology, Surat, India, (e-mail: mamulla@ieee.org).

Payal Patel is with the Department of Electrical Engineering, S. V. National Institute of Technology, Surat, India, (e-mail: pppatel1980@gmail.com).

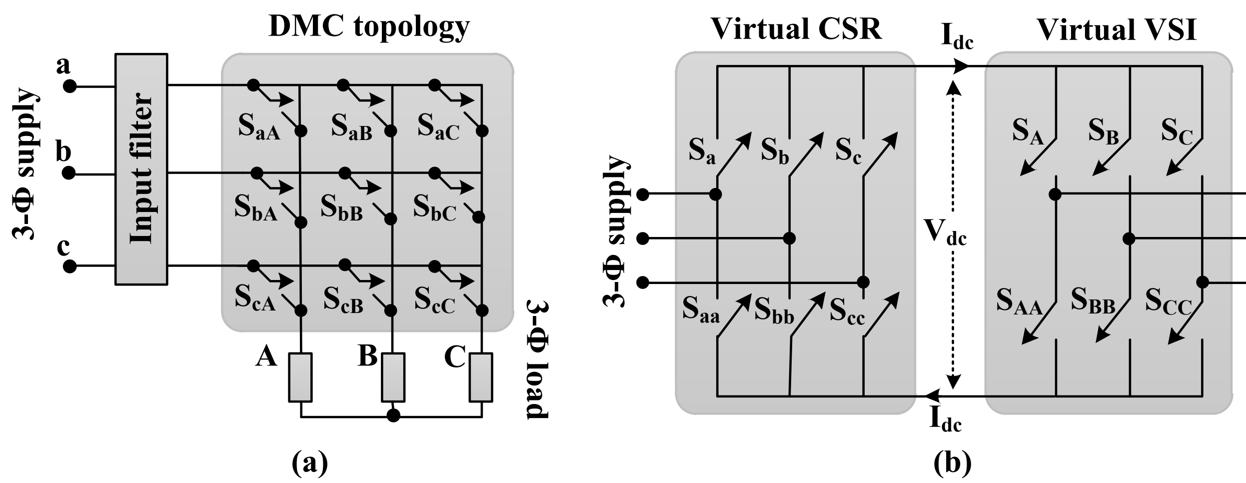

Fig. 1. (a) Matrix converter topology and (b) Indirect equivalent circuit of matrix converter

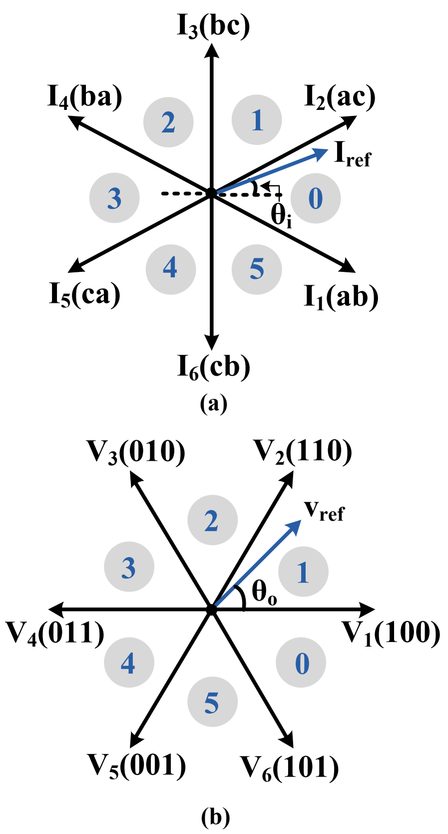

Fig. 2. Active switching vectors of (a) Rectifier and (b) Inverter stages

currents. Almost all above modulation techniques require the decomposition the positive/negative sequence components to enhance the supply current quality. However, the realization of decomposing positive/negative sequence components by the conventional methods suffers from the large storage requirements and/or high complexity.

This work proposes a new input current modulation technique for the MC to refine the quality of the supply currents under the conditions of unbalanced supply. The SVM technique upgrades the output performance of the MC by considering the actual input voltages as presented in [12][13]. The degraded quality of the supply currents in the above conditions is refined by the new input current modulation technique developed based on the principle of instantaneous power theory. The proposed technique modulates the input vector in the direction of the positive sequence vector of the supply voltages. Unlike the existing input modulation techniques, the presented technique realizes the above target by using the principle of dual p-q theory. The instantaneous oscillating powers are used to calculate the voltage components corresponding to negative sequence and harmonic components present in the supply voltages. The conventional approaches of decomposing sequence components for the existing input modulation techniques require large memory space and therefore difficult to realize in the practice. In this work, the performances of the MC are compared for the three different cases of input current modulations. The comparisons among the three cases are carried out based on the amount of harmonics present in the supply currents to prove the ability of new technique to upgrade the input performance of the MC. The results obtained by PSIM and OPAL-RT are presented to verify the effectiveness of the proposed input modulation technique.

This paper is organized in five sections. The modified SVM technique of the MC with the unbalanced supply voltages is explained in the section II. Section III explains the proposed input modulation technique. Simulation and real time simulation results are presented and discussed in section IV. Section V includes the conclusion of the work.

II. Space Vector Modulation of MC with Unbalanced Supply Voltages

In this section, the indirect SVM technique of the MC is explained. The SVM technique provides the required output performance under the unbalanced supply voltage conditions [13]. Fig. 1 (a) shows the topology of the MC consisting of nine bidirectional switches. The indirect SVM technique is derived using the indirect equivalent circuit of the MC as represented in Fig. 1 (b). The SVM techniques of the conventional rectifier and the inverter are applied to the input and output stages of the equivalent circuit of MC to calculate the duty cycles. The duty cycles of both stages are combined to obtain the duty cycles required to produce the switching pulses for the nine bidirectional switches of the MC topology [22].

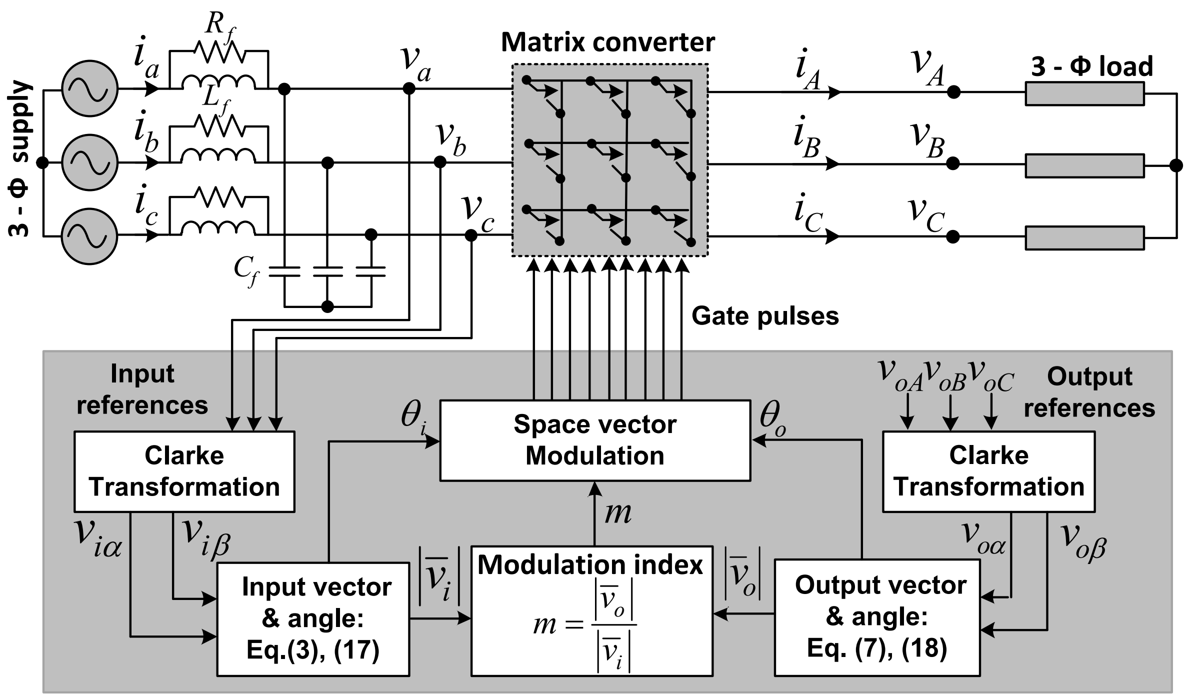

Fig. 3. MC modulation with the SVM technique

The modulations of the input and output stages of the MC using the SVM technique require the input angle θ_i, output angle θ_o and modulation index m. The conventional SVM technique of the MC does not incorporate the actual input voltage characteristics in the calculations of θ_i and m. As a result, the conventional SVM technique fails to produce the balanced output voltages in the presence of unbalanced and distorted power supply.

The modified SVM technique presented in [13] overcomes the above mentioned limitation of the conventional SVM technique by considering the actual characteristics of the supply voltages in the calculations of θ_i and m. As a result, the disturbances present in the supply voltages are compensated and balanced voltages are obtained at the output of the MC. The reference currents and voltages required to modulate the input and output stages of the indirect equivalent circuit are represented by Eq. (1) and Eq. (2) respectively. The reference currents are directly derived from the actual supply voltages v_a, v_b and v_c.

$$\begin{aligned} I_{ia} &= \sin \omega_i t \\ I_{ib} &= \sin\left(\omega_i t - \frac{2\pi}{3}\right) \\ I_{ic} &= \sin\left(\omega_i t + \frac{2\pi}{3}\right) \end{aligned} \tag{1}$$

where ω_i represents the angular frequency of the supply voltages. Here it is shown that the input reference currents follow the supply voltages as directly derived from it.

$$\begin{aligned} v_{oA} &= \sin \omega_o t \\ v_{oB} &= \sin\left(\omega_o t - \frac{2\pi}{3}\right) \\ v_{oC} &= \sin\left(\omega_o t + \frac{2\pi}{3}\right) \end{aligned} \tag{2}$$

where ω_o represents the required output angular frequency.

The six input and six output sectors associated with the modulations of the virtual input and output stages of the MC are shown in Fig. 2 (a) and (b), respectively. Figure 2 (a) represents the six active current vectors I_1-I_6 and three null vectors I_0 associated with the modulation of input rectifier stage in form of hexagon. Similarly, the hexagon formed by the six active voltage vectors V_1-V_6 and two zero vectors V_0 of the virtual output inverter stage of the MC are shown in Fig. 2 (b).

Fig. 3 shows the block diagram of the MC operation with the modified SVM technique considering the actual input voltages v_a, v_b and v_c. The input modulation angle θ_i is calculated using the $\alpha\beta$ components of these input voltages represented as $v_{i\alpha}$ and $v_{i\beta}$ as given by Eq. (3). The input angle θ_i decides the position of the input reference vector I_{ref} among the six input sectors. Let, I_{ref} is in sector-1 as shown in Fig. 2 (a). Based on this, the input vector I_{ref} is considered to be synthesized by impressing the adjoining active vectors I_1 and I_2 with duty cycles d_γ and d_δ respectively as calculated by Eq. (4)-(6).

$$\theta_i = tan^{-1}\frac{v_{i\beta}}{v_{i\alpha}} \tag{3}$$

$$I_{ref} = I_1 \cdot d_\gamma + I_2 \cdot d_\delta \tag{4}$$

$$d_\gamma = m_c \cdot \sin\left(\frac{\pi}{3} - \theta_r\right) \tag{5}$$

$$d_\delta = m_c \cdot \sin(\theta_r) \tag{6}$$

where m_c is the modulation index. $\theta_r = \theta_i - (S_r - 1)\cdot\frac{\pi}{3}$ is the angle which represents the position of I_{ref} in the respective input sector. S_r represents the input sector number.

Similarly, the output modulation angle θ_o is calculated using the $\alpha\beta$ components $v_{o\alpha}$ and $v_{o\beta}$ of the output reference voltages v_{oA}, v_{oB} and v_{oC} as given by Eq. (7). Let, the output reference vector is in sector-1 as shown in Fig. 2 (b). The corresponding equations of the output reference vector V_{ref} and duty cycles are given by Eq. (8)-(10).

$$\theta_o = tan^{-1}\frac{v_{o\beta}}{v_{o\alpha}} \tag{7}$$

$$V_{ref} = V_1 \cdot d_\alpha + V_2 \cdot d_\beta \tag{8}$$

$$d_\alpha = m_v \cdot \sin\left(\frac{\pi}{3} - \theta_v\right) \tag{9}$$

$$d_\beta = m_v \cdot \sin(\theta_v) \tag{10}$$

where m_v is the modulation index. $\theta_v = \theta_o - (S_v - 1)\cdot\frac{\pi}{3}$ is the angle which represents the position of V_{ref} in the respective output sector. S_v represents the output sector number.

The combined duty cycles of the MC are calculated by Eq. (11)-(15).

$$d_{\alpha\gamma} = d_\alpha \cdot d_\gamma = m \cdot \sin\left(\frac{\pi}{3} - \theta_v\right) \cdot \sin\left(\frac{\pi}{3} - \theta_i\right) \tag{11}$$

$$d_{\alpha\delta} = d_\alpha \cdot d_\delta = m \cdot \sin\left(\frac{\pi}{3} - \theta_v\right) \cdot \sin(\theta_i) \tag{12}$$

$$d_{\beta\gamma} = d_\beta \cdot d_\gamma = m \cdot \sin(\theta_v) \cdot \sin\left(\frac{\pi}{3} - \theta_i\right) \tag{13}$$

$$d_{\beta\delta} = d_\beta \cdot d_\delta = m \cdot \sin(\theta_v) \cdot \sin(\theta_i) \tag{14}$$

$$d_0 = 1 - d_{\alpha\gamma} - d_{\alpha\delta} - d_{\beta\gamma} - d_{\beta\delta} \tag{15}$$

where m is the overall modulation index of the MC as calculated by Eq. (16).

$$m = m_c.m_v = \frac{|v_o|}{|v_i|} \tag{16}$$

where $|v_i|$ and $|v_o|$ are obtained by the $\alpha\beta$ components of the actual input and the output reference voltages as represented by Eq. (17) and Eq. (18), respectively. The modulation index m in Eq. (16) assumes the variable amplitude for the abnormal supply voltage conditions. The m adjusts itself according to the actual characteristics of the supply voltages.

$$|v_i| = \sqrt{v_{i\alpha}^2 + v_{i\beta}^2} \tag{17}$$

$$|v_o| = \sqrt{v_{o\alpha}^2 + v_{o\beta}^2} \tag{18}$$

Thus, the modifications incorporated in the calculations of θ_i, θ_o and m according to the actual input voltages ensure the sinusoidal and balanced output waveforms in the unbalanced supply voltage conditions.

Nevertheless, the above condition introduces the large amount of lower order harmonics, esp. 3^{rd} and 5^{th}, into the supply currents degrading the quality of the supply as discussed previously [14]. This necessitates the use of any of the input modulation techniques suggested in[16], [15], [17] to use with the SVM technique to upgrade the supply current quality. These techniques make use of positive/negative sequence components of the supply voltages to derive the input references for the SVM technique. This helps in reducing the supply current harmonics when balanced voltages are generated at the output of the MC.

III. Proposed Input Modulation Technique

In this section, the new technique of deriving the input reference currents for the MC is developed to improve the supply current quality. This new technique is derived based on the dual p-q theory explained in [23] for 3-phase, 3-wire system. Section III-A explains the distribution of the harmonics in the MC supply currents due to the modified SVM technique. In Section III-B, the proposed technique of deriving the input modulation vector is explained in detail.

Consider the MC operation in the unbalanced supply voltage conditions. The MC produces the balanced output voltages using the modified SVM technique [12][13]. The supply voltages and currents to the MC in abc and $\alpha\beta$ reference frames are represented as follows:

$$v_{abc} = \begin{bmatrix} v_a \\ v_b \\ v_c \end{bmatrix} \xrightarrow{abc-\alpha\beta} v_{i\alpha\beta} = \begin{bmatrix} v_{i\alpha} \\ v_{i\beta} \end{bmatrix} \tag{19}$$

$$i_{abc} = \begin{bmatrix} i_a \\ i_b \\ i_c \end{bmatrix} \xrightarrow{abc-\alpha\beta} i_{i\alpha\beta} = \begin{bmatrix} i_{i\alpha} \\ i_{i\beta} \end{bmatrix} \tag{20}$$

where v_{abc} and i_{abc} are the supply voltage and current vectors in abc reference frame. $v_{i\alpha}$ and $v_{i\beta}$ are components of v_{abc} in $\alpha\beta$ reference frame. Similarly, $i_{i\alpha}$ and $i_{i\beta}$ are $\alpha\beta$ components of i_{abc}. The components $v_{i\alpha}$ and $v_{i\beta}$ can be represented as follows due to the unbalanced nature of the supply voltages.

$$v_{i\alpha} = v_{i\alpha_+} + v_{i\alpha_-} \tag{21}$$

$$v_{i\beta} = v_{i\beta_+} + v_{i\beta_-} \tag{22}$$

where $v_{i\alpha_+}$ and $v_{i\beta_+}$ represent the $\alpha\beta$ components of positive sequence supply voltages. Similarly, $v_{i\alpha_-}$ and $v_{i\beta_-}$ represent the $\alpha\beta$ components of negative sequence voltages present in the supply.

A. MC supply currents with the modified SVM technique under unbalanced supply voltage conditions

The MC performance is already examined in [12], [13], [14] for the unbalanced supply voltage conditions. The odd harmonics are introduced into the supply currents when the balanced load voltages are produced by the MC from the unbalanced supply [12]. Therefore, $i_{i\alpha}$ and $i_{i\beta}$ components of the supply currents can be represented in terms of positive sequence, negative sequence and harmonic components as follows:

$$i_{i\alpha} = i_{i\alpha_+} + i_{i\alpha_-} + i_{i\alpha_h} \tag{23}$$

$$i_{i\beta} = i_{i\beta_+} + i_{i\beta_-} + i_{i\beta_h} \tag{24}$$

where $i_{i\alpha_+}$ and $i_{i\beta_+}$ represent the $\alpha\beta$ components of the positive sequence supply currents. Similarly $i_{i\alpha_-}$, $i_{i\beta_-}$ and $i_{i\alpha_h}$, $i_{i\beta_h}$ represent the $\alpha\beta$ components of the negative sequence and harmonic components present in the supply currents respectively.

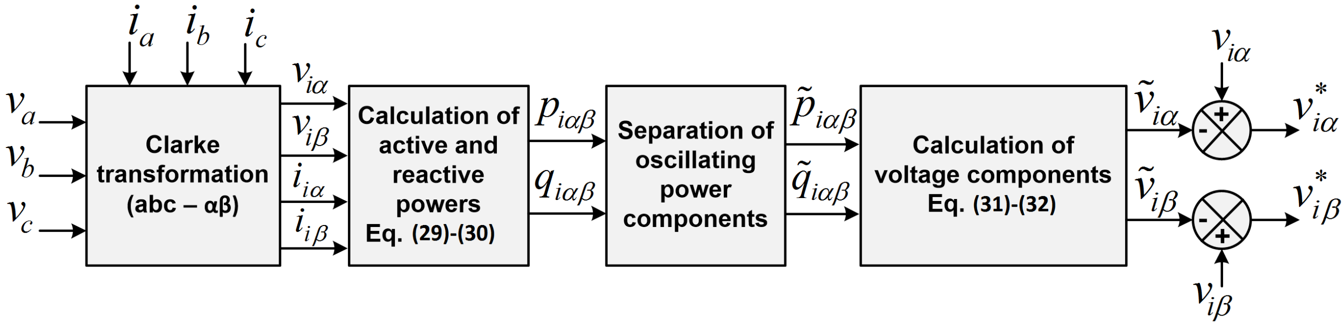

Fig. 4. Control diagram of deriving input modulation signals using proposed technique

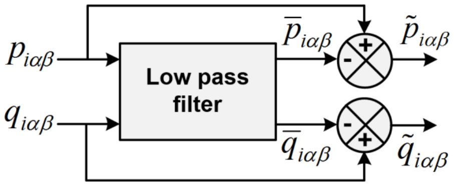

Fig. 5. Extraction of oscillating power components from the instantaneous active and reactive powers using low pass filter

B. Derivation of MC input modulation vector

The instantaneous p-q theory decomposes the current components corresponding to the various active and reactive power components. On the other hand, the voltage components corresponding to the various active and reactive power components are derived using the dual p-q theory [23]. Both these instantaneous theories are dual of each other. Recently, Farnaz et. al. presented the enhanced instantaneous power theory (EIPT) with the new approach of decomposing the various current components in the unbalanced and distorted supply conditions [24]. It is shown in [24] that, by using this oscillating power component and the voltage components, the unbalance and distorted components of the currents can be calculated. Using the similar approach and the duality, the present work develops the new technique of deriving the input reference vector for the MC under the unbalanced supply voltage condition. In this work, the unbalanced and distorted components of the voltages are calculated by using the supply current components and the instantaneous oscillating components of the power. Figure 4 shows the control diagram of the MC including the proposed input modulation technique.

The $\alpha\beta$ components of the supply voltages measured after the input filter are represented as follows:

$$v_{i\alpha} = v_{i\alpha_+} + v_{i\alpha_-} + v_{i\alpha_h} \tag{25}$$

$$v_{i\beta} = v_{i\beta_+} + v_{i\beta_-} + v_{i\beta_h} \tag{26}$$

where $v_{i\alpha_h}$ and $v_{i\beta_h}$ represent the harmonic components injected into the supply voltages as a result of the voltage drop across the source and filter impedance by the distortion in the supply currents. However, the amount of these harmonic components is very small.

According to the instantaneous power theory, the active and reactive powers are calculated using the $\alpha\beta$ components of the supply voltages and currents as given below:

$$p_{i\alpha\beta} = v_{i\alpha} i_{i\alpha} + v_{i\beta} i_{i\beta} \tag{27}$$

$$q_{i\alpha\beta} = v_{i\beta} i_{i\alpha} - v_{i\alpha} i_{i\beta} \tag{28}$$

where $p_{i\alpha\beta}$ and $q_{i\alpha\beta}$ represent the instantaneous active and reactive powers.

The instantaneous active and reactive powers are represented in terms of average and oscillating components as given by Eq. (29) and (30). The presence of the oscillating term in the power is due to the unbalance present in the power supply.

$$p_{i\alpha\beta} = \overline{p}_{i\alpha\beta} + \tilde{p}_{i\alpha\beta} \tag{29}$$

$$q_{i\alpha\beta} = \overline{q}_{i\alpha\beta} + \tilde{q}_{i\alpha\beta} \tag{30}$$

where $\overline{p}_{i\alpha\beta}$ and $\overline{q}_{i\alpha\beta}$ represent the average active and reactive power components, respectively. The oscillating components of the active and reactive powers are represented by $\tilde{p}_{i\alpha\beta}$ and $\tilde{q}_{i\alpha\beta}$, respectively.

The oscillating power components are extracted from the instantaneous active and reactive powers using the low pass filter as shown in the Fig. 5. The oscillating power terms $\tilde{p}_{i\alpha\beta}$ and $\tilde{q}_{i\alpha\beta}$ are separated by subtracting the average power components $\overline{p}_{i\alpha\beta}$ and $\overline{q}_{i\alpha\beta}$ obtained at the output of the low pass filter from $p_{i\alpha\beta}$ and $q_{i\alpha\beta}$, respectively. Based on the principle of dual p-q theory and the formulations of the current components in EIPT presented in [24], the voltage components corresponding to the oscillating power components $\tilde{p}_{i\alpha\beta}$ and $\tilde{q}_{i\alpha\beta}$ are calculated using the Eq. (31) and Eq. (32).

$$\tilde{v_{i\alpha}} = \frac{i_{i\alpha}}{i_{i\alpha}^2 + i_{i\beta}^2}\tilde{p}_{i\alpha\beta} + \frac{i_{i\beta}}{i_{i\alpha}^2 + i_{i\beta}^2}\tilde{q}_{i\alpha\beta} \tag{31}$$

$$\tilde{v_{i\beta}} = \frac{i_{i\beta}}{i_{i\alpha}^2 + i_{i\beta}^2}\tilde{p}_{i\alpha\beta} - \frac{i_{i\alpha}}{i_{i\alpha}^2 + i_{i\beta}^2}\tilde{q}_{i\alpha\beta} \tag{32}$$

where $\tilde{v_{i\alpha}}$ and $\tilde{v_{i\beta}}$ represent the unbalanced and distorted voltage components of the supply voltages. As the amount of harmonics is small in the supply voltages, these oscillating voltage components $\tilde{v_{i\alpha}}$ and $\tilde{v_{i\beta}}$ dominated with the negative sequence components of the supply voltages. $\tilde{v_{i\alpha}}$ and $\tilde{v_{i\beta}}$ are represented by Eq. (33) and (34).

$$\tilde{v_{i\alpha}} = v_{i\alpha_-} + v_{i\alpha_h} \tag{33}$$

$$\tilde{v_{i\beta}} = v_{i\beta_-} + v_{i\beta_h} \tag{34}$$

Now, the input modulation vector components $v_{i\alpha}^*$ and $v_{i\beta}^*$ are derived by subtracting the oscillating voltage components $\tilde{v_{i\alpha}}$ and $\tilde{v_{i\beta}}$ from the supply voltage components $v_{i\alpha}$ and $v_{i\beta}$ as represented by following expressions:

$$v_{i\alpha}^* = v_{i\alpha} - \tilde{v_{i\alpha}} = v_{i\alpha_+} \tag{35}$$

$$v_{i\beta}^* = v_{i\beta} - \tilde{v_{i\beta}} = v_{i\beta_+} \tag{36}$$

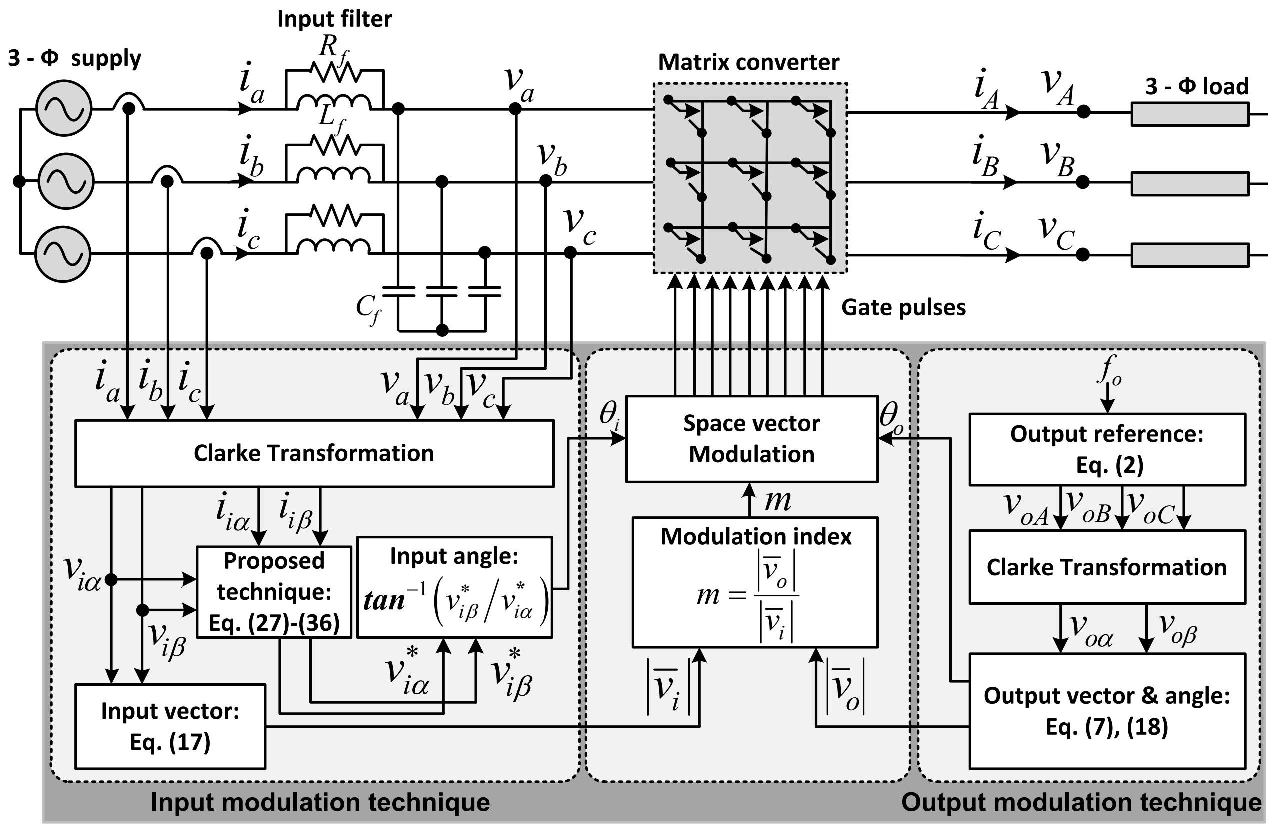

Fig. 6. Block diagram of MSVM modulated MC with proposed input modulation technique

It is shown that the $\alpha\beta$ components of the input modulation vector contain only the positive sequence components of the supply voltages. This is similar to the well established input modulation technique presented in [17][18] which utilizes the positive sequence components of the supply voltages for the input modulation of the MC. Therefore, the proposed technique is expected to provide the performance similar to that obtained with the input modulation scheme of [17][18]. The presented approach of deriving the input modulation vector does not need complex and memory consuming sequence decomposition methods which leads to the easy implementation. Now, $v^*_{i\alpha}$ and $v^*_{i\beta}$ are used in Eq. (3) and (17) instead of $v_{i\alpha}$ and $v_{i\beta}$ to calculate the input reference vector and input angle, respectively as represented by Eq. (37) and (38), respectively.

$$|v_i| = \sqrt{{v^*}^2_{i\alpha} + {v^*}^2_{i\beta}} \tag{37}$$

$$\theta_i = tan^{-1}\frac{v^*_{i\beta}}{v^*_{i\alpha}} \tag{38}$$

Figure 6 shows the modified SVM scheme to control the MC with the proposed input modulation technique in the unbalanced supply voltage conditions.

IV. Results and Discussion

In this section, the performance of the MC modulated with the SVM technique is evaluated by applying new input modulation technique in the presence of unbalanced supply voltages. The MC performances for the three different cases are compared in order to verify the effectiveness of the new input current modulation technique. The supply current qualities of the MC for the three cases are compared based on the amount of harmonics. Case-1 includes the operation of the MC with the SVM technique without modifying the input modulation vector [13]. In case-2, the input reference vector is modulated in the same direction to that of positive sequence vector of the supply voltages [17]. In this case, the positive sequence components are decomposed using the Fortescue theorem. In Case-3, the input reference vector is derived using the proposed input current modulation technique. The simulations are performed in the PSIM environment. The system parameters in the simulation are chosen according to the Table I. The real time results for the MC are obtained by the OPAL-RT integrated with MATLAB/Simulink. The setup of OPAL-RT integrated with MATLAB/Simulink is shown in Fig. 7. The real time simulation parameters are shown in Table II.

TABLE I
Simulation parameters

System parameter	Description	Value
Source parameters	Frequency (f_i)	50 Hz
Filter parameters	Inductor (L_f)	2 mH
	Capacitor (C_f)	18 μF
	Resistance (R_f)	58 Ω
Load parameters	Resistance (R_L)	10 Ω
	Inductance (L_L)	10 mH
Control parameters	Carrier frequency (f_c)	5 kHz

The comparison of the MC performance for the above three cases is carried out in the presence of unbalanced

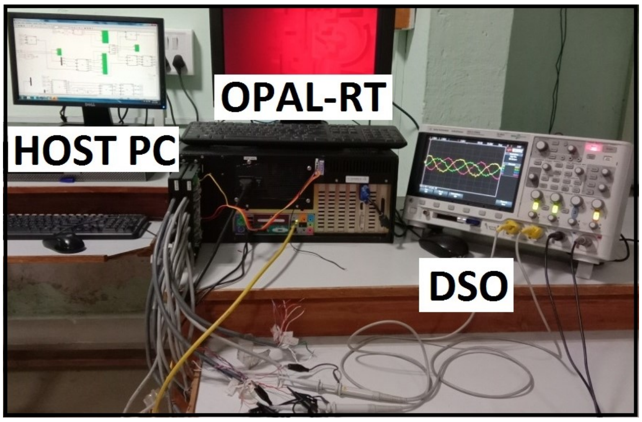

Fig. 7. Real time simulation set up using OPAL-RT

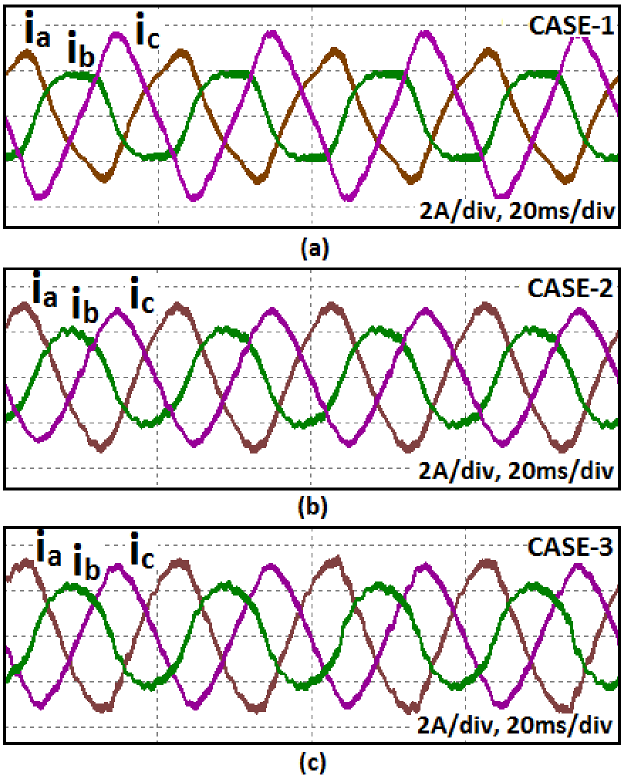

Fig. 8. Simulation results of supply currents: (a) Case-1 (b) Case-2 and (c) Case-3

TABLE II
REAL TIME SIMULATION PARAMETERS

System parameter	Description	Value
Source parameters	Frequency (f_i)	50 Hz
Filter parameters	Inductor (L_f)	5 mH
	Capacitor (C_f)	15 μF
	Resistance (R_f)	48 Ω
Load parameters	Resistance (R_L)	15 Ω
	Inductance (L_L)	15 mH
Control parameters	Carrier frequency (f_c)	3.7 kHz

supply voltages as given in Eq. (39).

$$\begin{aligned} v_a &= v_m \sin(\omega_i t) \\ v_b &= 0.7 v_m \sin(\omega_i t - 2\pi/3) \\ v_c &= 1.4 v_m \sin(\omega_i t + 2\pi/3) \end{aligned} \tag{39}$$

where the values of v_m and f are chosen to be $255\sqrt{2}$ V and 50 Hz respectively.

As the MC is controlled by SVM technique by considering the actual supply voltages, the balanced output currents are expected in all three cases. The input performances of the MC are evaluated based on the amount of harmonics present in the supply currents. The index terms used to analyze the presence of the harmonics in the supply currents are: harmonic distortion (*HD*), frequency weighted harmonic distortion (*FHD*) and total harmonic distortion (*THD*). The expressions of *HD*, *FHD* and *THD* are given below [17],

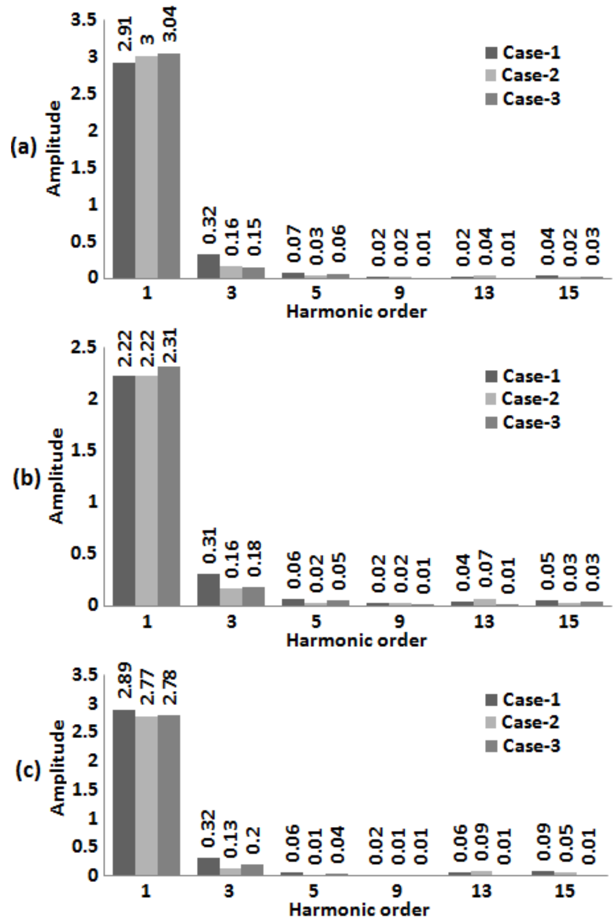

Fig. 9. Harmonic spectrums of simulated supply currents for the three cases: (a) Phase-a (b) Phase-b and (c) Phase-c

$$HD = \frac{\sqrt{\sum_{h=3,5..}^{\infty} i_h}}{i_1} \tag{40}$$

$$FHD = \frac{\sqrt{\sum_{h=3,5..}^{\infty} (i_h/h)}}{i_1} \tag{41}$$

$$THD = \frac{\sqrt{\sum_{h=3,5..}^{\infty} i_h^2}}{i_1} \tag{42}$$

where h, i_h and i_1 represent the order of the harmonic, magnitude of the harmonic and fundamental supply current components respectively.

The simulation results of the supply currents for the case-1, 2 and 3 are shown in the Fig. 8. It is observed that the supply currents in case-1 are much more distorted as compared to case-2 and case-3. Fig. 12 includes the harmonic spectrums of the supply currents obtained in the three cases. Fig. 10 compares the supply currents of the MC for the three cases on the basis of %*HD*, %*FHD* and %*THD*. The comparison carried out in terms of %*HD* is shown in Fig. 10 (a). The %*HD* of the supply currents in case-1 are highest

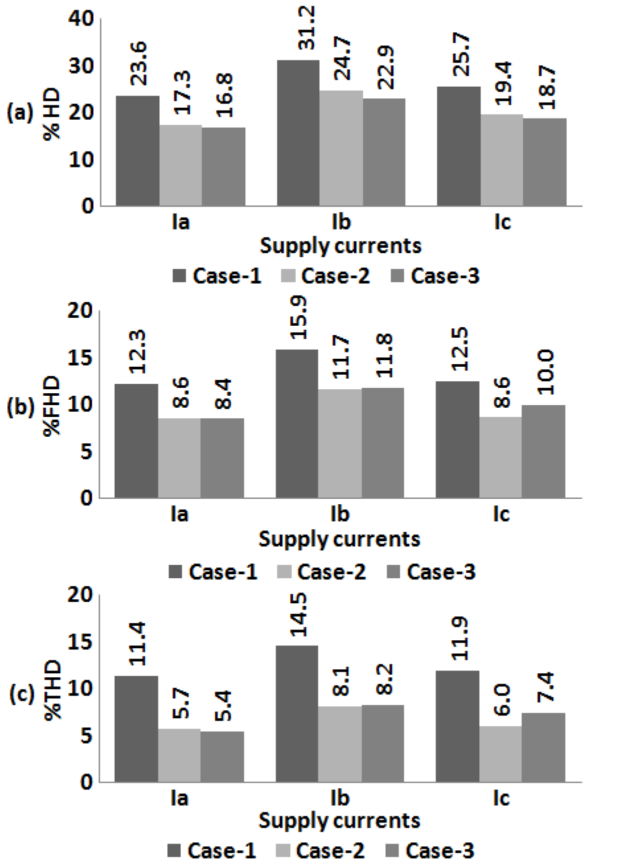

Fig. 10. Comparison of simulated supply currents based on: (a)%HD, (b)%FHD and (c)%THD

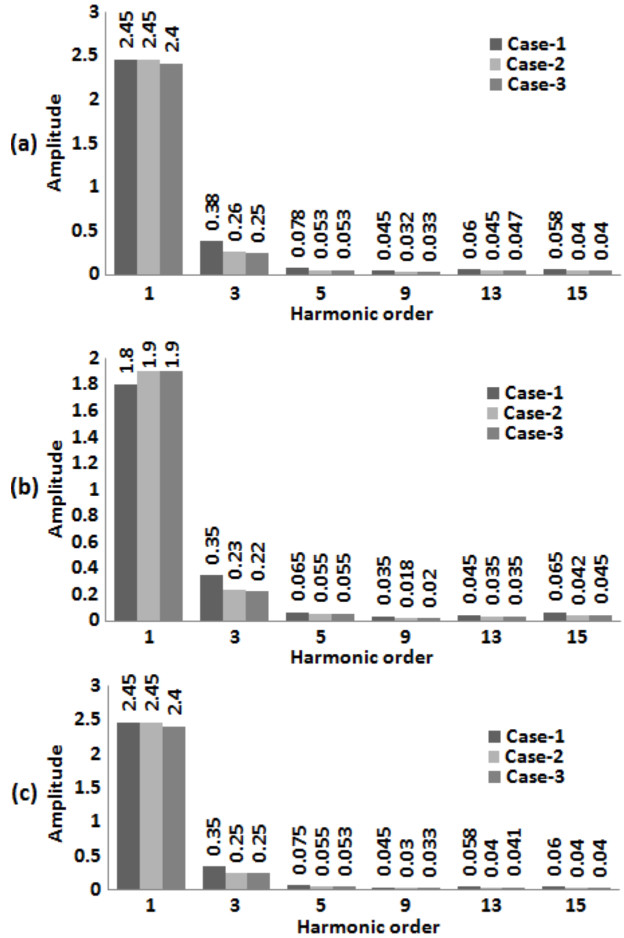

Fig. 12. Harmonic spectrums of experimental supply currents for the three cases: (a) Phase-a (b) Phase-b and (c) Phase-c

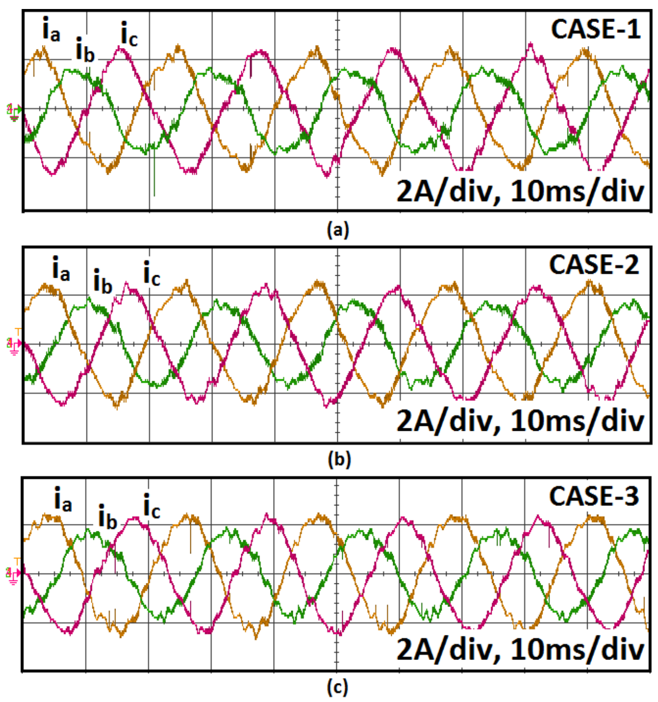

Fig. 11. Experimental results of the supply currents: (a) case-1 (b) case-2 and (c) case-3

whereas lowest in case-3. In Fig. 10 (b), the supply currents are compared based on the $\%FHD$. The $\%FHD$ are highest for the supply currents in case-1 and lowest for the supply currents of case-3. However, there is no major difference between the performances of the supply currents in case-2 and case-3. Fig. 10 (c) represents the comparison of MC supply currents for the three cases based on $\%THD$. Case-1 provides the highest $\%THD$ of the supply currents. The supply current $\%THD$s are nearly equal in case-2 and 3 and are remarkably lower than case-1. Comparison of the MC input performances in the above three cases prove the potential of the new technique to upgrade the supply current quality. The real time results of the MC supply currents obtained for the three above cases are shown in Fig. 11. The harmonic spectrums of these experimental supply currents are compared in Fig. 12. Fig. 13 shows the comparison of these currents based on$\%HD$, $\%FHD$ and $\%THD$. These results also prove the ability of the proposed technique to reduce the harmonics from the supply currents in the presence of unbalance supply. The performance exhibited by this new technique is approximately similar to that of the performance obtained in case-2.

Fig. 14 shows the load current waveforms of the MC obtained in the three cases. It is observed that the output currents are balanced and nearly sinusoidal in the nature. The comparisons of the load currents for the three cases are presented in Fig. 15 (a) and (b) based on $\%THD$ and peak amplitude of the fundamental components, respectively. The value of $\%THD$ is approximately 5% for the load currents in all the three cases. Also, the peak amplitudes of the load currents in three cases are approximately same. This proves the effectuality of SVM technique to yield the balanced and

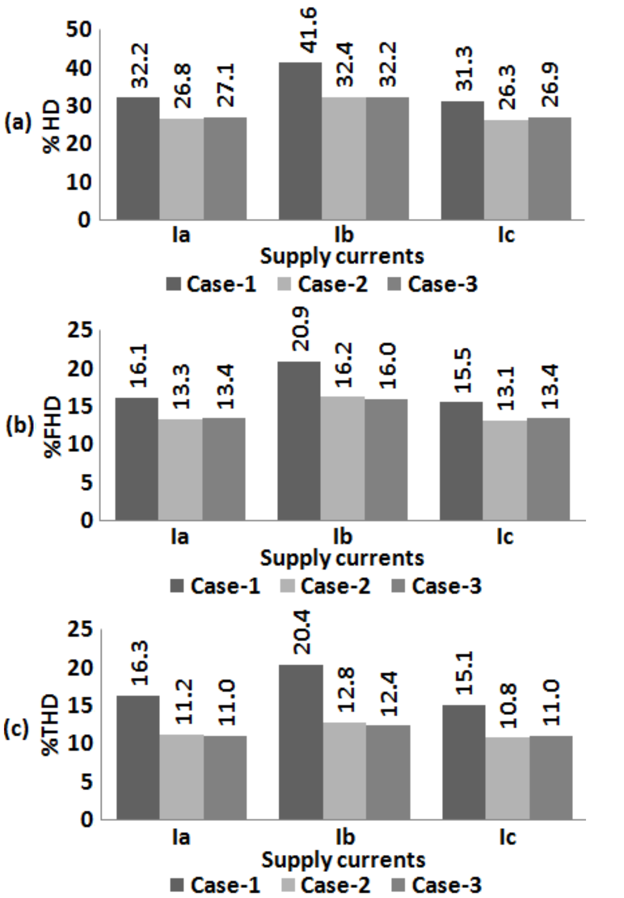

Fig. 13. Comparison of experimental supply currents based on: (a)%HD, (b)%FHD and (c)%THD

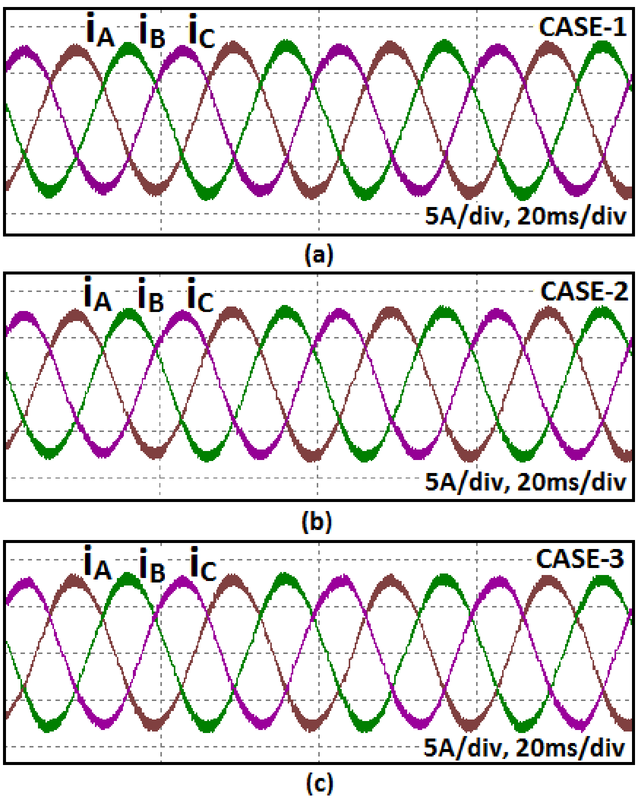

Fig. 14. Simulation results of load currents: (a) case-1 (b) case-2 and (c) case-3

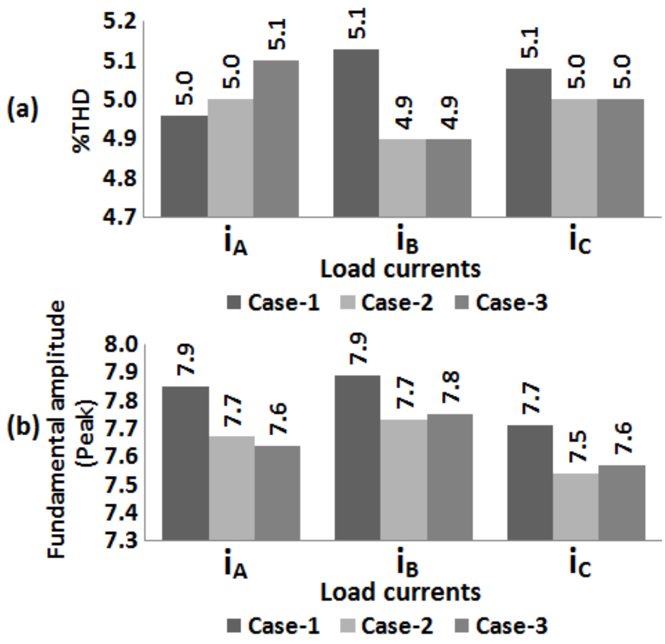

Fig. 15. Comparison of simulated load currents based on: (a) %THD and (b) peak amplitude of fundamental component

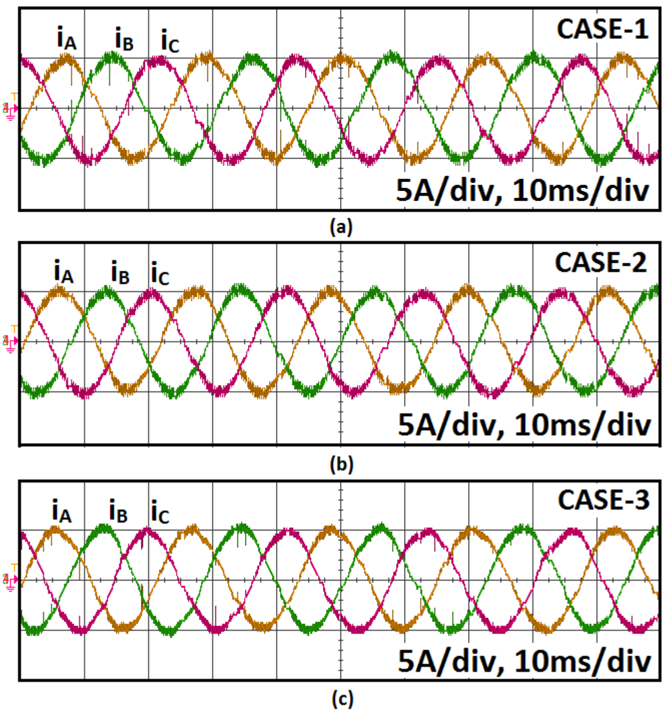

Fig. 16. Experimental results of the load currents: (a) case-1 (b) case-2 and (c) case-3

sinusoidal output currents in the presence of unbalanced supply voltages. The real time results of load currents for the three considered cases are represented in Fig. 16 which are approximately similar to the simulation results. Fig. 17 (a) and (b) represent the $\%THD$ and peak amplitudes of the fundamental components of the experimentally obtained load currents, respectively. Approximately 6.5 $\%THD$ and 5 V peak amplitudes are obtained for the load currents in all the three cases.

The simulation and the real time results of the output line voltages obtained in case-3 are shown in Fig. 18 and

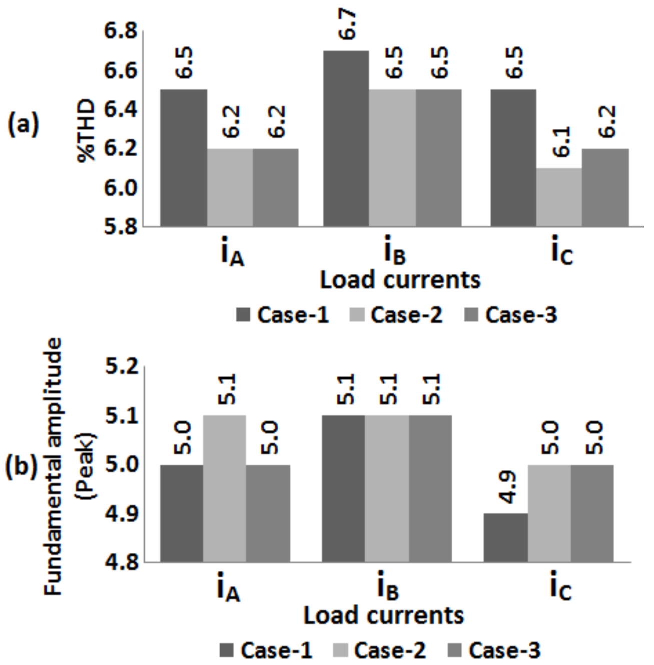

Fig. 17. Comparison of experimental load currents based on: (a) %THD and (b) peak amplitude of fundamental component

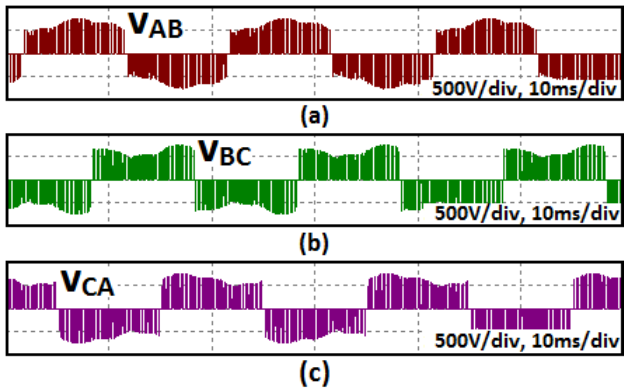

Fig. 18. Simulation results of balanced load voltages (line) produced by SVM technique

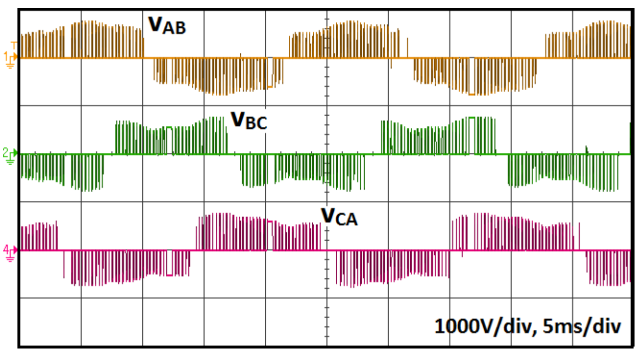

Fig. 19. Experimental results of load voltages (line) produced by MSVM technique

Fig. 19, respectively. Figure 20 shows the comparison of the fundamental components of the output line voltages obtained by the simulation and the experiment. It is shown that the peak amplitudes of all output line voltages are approximately 140 V. This shows that the improvement in the supply currents by the proposed technique does not affect the generation of the ability of the SVM technique to provide

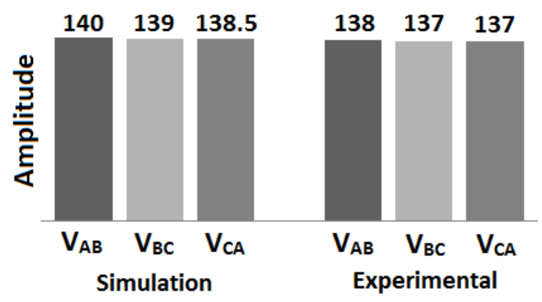

Fig. 20. Comparison of the fundamental amplitudes of the output line voltages obtained by the simulation and experiment.

the balanced output voltages for the MC.

The comparison of the MC input performance under the unbalanced supply conditions proves the ability of the presented new input modulation technique to reduce the supply current harmonics. It is observed that the harmonics in the supply currents are reduced up to the considerable amount in case-2 and case-3 in comparison with the case-1. The output performance of the MC in case-3 is not affected by the new input modulation technique similar to case-1 and case-2.

V. Conclusion

This work introduces the new input current modulation technique for the MC. The new technique improves the supply current quality of the MC when the supply voltages are unbalanced. The new technique developed on the concept of dual p-q theory modulates the input reference vector of the MC in the same direction to that of positive sequence components of the supply. The presented technique calculates the voltage components corresponding to the oscillating power components of the total instantaneous power to derive the input modulation vector of the MC. These voltage components correspond to the negative sequence and harmonic components present in the supply voltages. This is different from most of the existing input modulation techniques which are highly dependent on the sequence decomposition algorithms requiring the large storage space for the realization. The harmonics present in the supply currents are successfully reduced by the new input modulation technique without affecting the output performance of the MC. The presented work is validated by the simulation results obtained in PSIM and test results of real-time simulations performed in OPAL-RT.

References

[1] L. Empringham, J. W. Kolar, J. Rodriguez, P. W. Wheeler, and J. C. Clare, "Technological issues and industrial application of matrix converters: A review," *IEEE Transactions on Industrial Electronics*, vol. 60, no. 10, pp. 4260–4271, 2013.

[2] L. Huber and D. Borojevic, "Space vector modulated three-phase to three-phase matrix converter with input power factor correction," *IEEE transactions on industry applications*, vol. 31, no. 6, pp. 1234–1246, 1995.

[3] Sirichai and Tammaruckwattana, "Modeling and simulation of wind power generation system using ac to ac converter," *International MultiConference of Engineers and Computer Scientists (IMECS)*, vol. 2, pp. 593–597, March 16-18, 2016.

[4] H. Karaca and R. Akkaya, "Control of venturini method based matrix converter in input voltage variations," *International MultiConference of Engineers and Computer Scientists (IMECS)*, vol. 2, March 18-20, 2009.

[5] P. Enjeti and X. Wang, "A critical evaluation of harmonics generated by forced commutated cycloconverters (fcc's) under unbalance," in *[Proceedings] IECON'90: 16th Annual Conference of IEEE Industrial Electronics Society*. IEEE, 1990, pp. 1162–1168.

[6] A. Dastfan and M. Haghshenas, "Design and simulation of a power supply based on a matrix converter under unbalanced input voltage," in *Universities Power Engineering Conference, 2006. UPEC'06. Proceedings of the 41st International*, vol. 2. IEEE, 2006, pp. 569–573.

[7] L. Zhang, C. Watthanasarn, and W. Shepherd, "Control of ac-ac matrix converters for unbalanced and/or distorted supply voltage," in *2001 IEEE 32nd Annual Power Electronics Specialists Conference (IEEE Cat. No. 01CH37230)*, vol. 2. IEEE, 2001, pp. 1108–1113.

[8] H. Karaca, R. Akkaya, and H. Dogan, "A novel compensation method based on fuzzy logic control for matrix converter under distorted input voltage conditions," in *2008 18th International Conference on Electrical Machines*. IEEE, 2008, pp. 1–5.

[9] C. Xiyou, C. Xueyun, and W. Qi, "The improvement of space vector modulation strategy for matrix converter under unbalanced input voltages," *Transactions of China Electrotechnical Society*, vol. 15, no. 2, pp. 78–82, 2000.

[10] M. Jussila and H. Tuusa, "Comparison of simple control strategies of space-vector modulated indirect matrix converter under distorted supply voltage," *IEEE Transactions on Power Electronics*, vol. 22, no. 1, pp. 139–148, 2007.

[11] P. Nielsen, F. Blaabjerg, and J. K. Pedersen, "Space vector modulated matrix converter with minimized number of switchings and a feedforward compensation of input voltage unbalance," in *Power Electronics, Drives and Energy Systems for Industrial Growth, 1996., Proceedings of the 1996 International Conference on*, vol. 2. IEEE, 1996, pp. 833–839.

[12] X. Wang, H. Lin, H. She, and B. Feng, "A research on space vector modulation strategy for matrix converter under abnormal input-voltage conditions," *IEEE Transactions on Industrial Electronics*, vol. 59, no. 1, pp. 93–104, 2012.

[13] P. Patel and M. A. Mulla, "Modified space vector modulated three-phase to three-phase matrix converter under unbalanced supply conditions," in *2018 8th IEEE India International Conference on Power Electronics (IICPE)*. IEEE, 2018, pp. 1–6.

[14] D. Casadei, G. Serra, and A. Tani, "A general approach for the analysis of the input power quality in matrix converters," *IEEE Transactions on Power Electronics*, vol. 13, no. 5, pp. 882–891, 1998.

[15] F. Blaabjerg, D. Casadei, C. Klumpner, and M. Matteini, "Comparison of two current modulation strategies for matrix converters under unbalanced input voltage conditions," *IEEE Transactions on Industrial Electronics*, vol. 49, no. 2, pp. 289–296, 2002.

[16] D. Casadei, G. Serra, and A. Tani, "Reduction of the input current harmonic content in matrix converters under input/output unbalance," *IEEE Transactions on Industrial Electronics*, vol. 45, no. 3, pp. 401–411, 1998.

[17] P. Patel and M. A. Mulla, "Supply current quality improvement for three-phase matrix converter under unbalanced supply voltage conditions," in *2018 IEEE International Conference on Power Electronics, Drives and Energy Systems (PEDES)*. IEEE, 2018, pp. 1–6.

[18] X. Li, M. Su, Y. Sun, H. Dan, and W. Xiong, "Modulation strategies based on mathematical construction method for matrix converter under unbalanced input voltages," *IET Power Electronics*, vol. 6, no. 3, pp. 434–445, 2013.

[19] Y. Yan, H. An, T. Shi, and C. Xia, "Improved double line voltage synthesis of matrix converter for input current enhancement under unbalanced power supply," *IET Power Electronics*, vol. 6, no. 4, pp. 798–808, 2013.

[20] J. Lei, B. Zhou, J. Bian, X. Qin, and J. Wei, "A simple method for sinusoidal input currents of matrix converter under unbalanced input voltages," *IEEE Transactions on Power Electronics*, vol. 31, no. 1, pp. 21–25, 2015.

[21] J. Lei, B. Zhou, J. Bian, J. Wei, Y. Zhu, J. Yu, and Y. Yang, "Feedback control strategy to eliminate the input current harmonics of matrix converter under unbalanced input voltages," *IEEE Transactions on Power Electronics*, vol. 32, no. 1, pp. 878–888, 2016.

[22] P. Patel and M. A. Mulla, "Space vector modulated three-phase to three-phase direct matrix converter," in *2016 IEEE 16th International Conference on Environment and Electrical Engineering (EEEIC)*. IEEE, 2016, pp. 1–6.

[23] H. Akagi, E. H. Watanabe, and M. Aredes, *Instantaneous power theory and applications to power conditioning*. John Wiley & Sons, 2017.

[24] F. Harirchi and M. G. Simoes, "Enhanced instantaneous power theory decomposition for power quality smart converter applications," *IEEE Transactions on Power Electronics*, vol. 33, no. 11, pp. 9344–9359, 2018.